Korean Journal of Remote Sensing, Vol.26, No.3, 2010, pp.297~304

Velocity Estimation of Moving Targets on the Sea Surface by Azimuth Differentials of Simulated-SAR Image

Chan-Su Yang*†, Youn-Seop Kim*, and Kazuo Ouchi**

*Ocean Satellite Research Center, Korea Ocean Research & Development Institute

**Department of Computer Science, National Defense Academy

Abstract : Since the change in Doppler centroid according to moving targets brings alteration to the phase in azimuth differential signals of synthetic aperture radar (SAR) data, one can measure the velocity of the moving targets using this effect. In this study, we will investigate theoretically measuring the velocity of an object from azimuth differential signals by using range compressed data which is the interim outcome of treatment from the simulated SAR raw data of moving targets on the background of sea clutter. Also, it will provide evaluation for the elements that affect the estimation error of velocity from a single SAR sensor. By making RADARSAT-1 simulated image as a specific case, the research includes comparisons for the means of velocity measurement classified by the directions of movement in the four following cases. 1. A case of a single target without currents, 2. A case of a single target with tidal currents of 0.5 m/s, 1 m/s, and 3 m/s, 3. A case of two targets on a same azimuth line moving in a same direction and velocity, 4. A case of a single target contiguous to land where radar backscatter is strong.

As a result, when two moving targets exist in SAR image outside the range of approximately 256 pixels, the velocity of the object can be measured with high accuracy. However, when other moving targets exist in the range of approximately 128 pixels or when the target was contiguous to the land of strong backscatter coefficient (NRCS: normalized radar cross section), the estimated velocity was in error by 10% at the maximum. This is because in the process of assuming the target's location, an error occurs due to the differential signals affected by other scatterers.

Key Words : Velocity estimation, Moving target, Sea clutter, Simulated-SAR image.

1. Introduction

With a large coverage, short repeatability, day and night, and all weather observation capability, Synthetic Aperture Radar (SAR) has been proven to be a very effective tool for environmental monitoring, and is expected to result in numerous scientifically valuable and commercially feasible applications. In SAR processing, scatterers are assumed to be stationary during the time of aperture synthesis in azimuth direction, and therefore, if scatterers move, they cause errors in the SAR images, including defocusing and image displacement, depending on the direction of their motion [1, 2, 3].

Received January 21, 2010; Revised June 14, 2010; Accepted June 21, 2010.

† Corresponding Author: Chan-Su Yang (yangcs@kordi.re.kr)

A well-known effect of scatterers' motion is azimuth image shift caused by the slant-range velocity component. Since detection, identification and tracking of moving objects in SAR signals are important in both civil and military applications, the errors need to be corrected.

As an ocean application of SAR, the azimuth shift can be used to calculate the velocity of moving vessels. The determination of the ship velocity from the displacement (shift) between ship and its wake is a typical example [4, 5]. With increasing importance in monitoring ship traffic in both coastal and open ocean, an automatic algorithm for the detection of ships, wakes, and cruising velocity is very desirable. Ship wakes, which appear in a form of bright and dark streaks in SAR images, rely on the ship speed, type, size and so on. However, SAR images do not always reveal ship wakes.

Several methods have been proposed to detect and focus moving targets using a single antenna. Most of them are based on the cross-range phase history originated by moving targets [6, 7, 8, 9, 10, 11].

In this paper, a theoretical investigation for detection of moving targets and for estimation of their velocities is presented using simulation SAR images by differentiating range-processed raw data in terms of azimuth time. In the second part of the paper, the basic theory of velocity estimation from azimuth differential signals is described, followed by the generation of simulated SAR raw data in section 3. In section 4, velocity estimation is carried out using the simulated raw data with and without the background currents, and the case of multiple targets is considered in section 5. Finally, the results are summarized in section 6.

2. Estimation Algorithm of Target Velocity Using Azimuth Differential Signal

Fig. 1 illustrates the SAR geometry where a point scatterer is moving in the ground-range direction with velocity V_R. The return signal in the azimuth direction can be expressed by the following equation [12].

$$E_R(t) = E_o(R)\exp(-i\frac{4\pi}{\lambda}r(t)) \tag{1}$$

where $E_o(R)$ is the signal amplitude on a datum point whose distance from the radar is R, λ is the wavelength of SAR, and $r(t)$ means the slant-range distance between the moving target and the radar at azimuth time t.

If the target's radar radial velocity is V_{SR}, $r(t)$ can be expressed as the following equation.

$$\begin{aligned} r(t) &= ((R + V_{SR}t)^2 + V^2t^2)^{1/2} \\ &\approx R + V_{SR}t + V^2t^2 / 2R \end{aligned} \tag{2}$$

where V is the platform velocity, V_{SR} is related to V_R, by $V_{SR} = V_R \sin\theta$, and θ is the incidence angle.

Azimuth differential signals at times t and t_c are as follows when they are evaluated using equation (1) and equation (2).

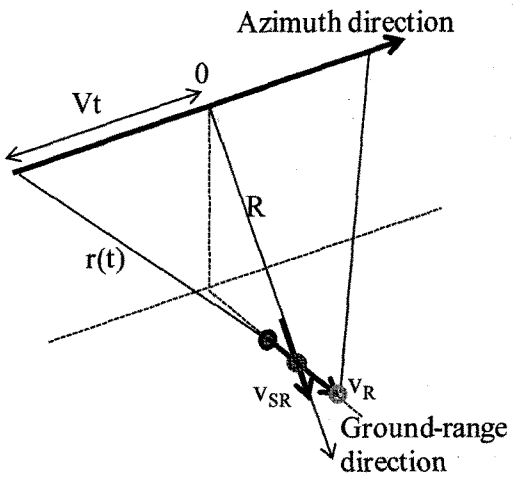

Fig. 1. SAR geometry for a moving target.

$$\Delta E = E_R(t_C)E_R^*(t)$$
$$= |E_o(R)|^2 \exp\left(-i\frac{4\pi}{\lambda}\left(V_{SR}(t_C - t) + \frac{V^2}{2R}(t_C^2 - t^2)\right)\right) \quad (3)$$
$$= |E_o|^2 \exp\left(-i\frac{4\pi}{\lambda}\left(V_{SR}\Delta t + \frac{V^2\Delta t^2}{2R} + \frac{V^2\Delta t}{R}t\right)\right)$$

where $\Delta t = t_c - t$, and in this paper, Δt is defined as the time equivalent to 1 pixel in the azimuth direction (Δt = 1/PRF).

From equation (3), the phase $\Delta\phi$ of azimuth differential signals can be expressed as

$$\Delta\phi = \arctan\left(\frac{\mathrm{Im}\{\Delta E\}}{\mathrm{Re}\{\Delta E\}}\right)$$
$$= -\frac{4\pi}{\lambda}\left(V_{SR}\Delta t + \frac{V^2\Delta t^2}{2R}\right) - \frac{4\pi}{\lambda}\frac{V^2\Delta t}{R}t + 2n\pi, \quad (4)$$
$$n = 0, pm1, pm2,$$

In equation (4), since the second and third terms on the right hand can be calculated from SAR parameters, the target's slant-range velocity V_{SR} can be estimated from the remaining phase after eliminating the second and third terms. For example, the differential phases can be plotted with V_{SR} along azimuth pixels, calculated for moving targets as shown in Fig. 2. The sloped lines represent the speeds of moving targets for the cases of V_{SR} = -10 m/s and 10 m/s. The differential phase of y axis is a constant proportional to the range velocity of the target.

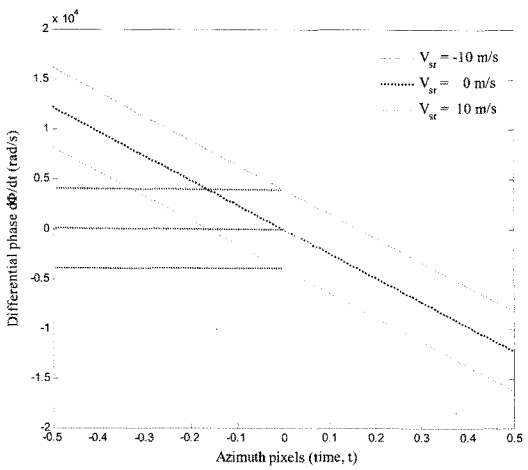

Fig. 2. Differential phases as a function of azimuth pixels and range velocities of target moving with -10 m/s and 10 m/s.

3. Generation of SAR Raw Data

In the paper, strip-map mode that forms a continuous strip of imagery parallel to the platform's flight path is applied among several SAR operation modes according to how to obtain images. In the simulation study, we produce two-dimensional SAR raw data using the RADARSAT-1 strip-map mode of which the parameters are listed in Table 1. The delay times, τ and t denote the slant-range and azimuth times, respectively.

The general form demodulated for received signal from scatterers is expressed as follows (Runge and Bamler, 1992; Raney *et al.*, 1994; Yeo *et al.*, 2001).

$$pp(\tau,t;r_s) = \sigma \cdot a(t;r_s)s_o\left[\tau - \frac{2R(t;r_s)}{c}\right] \cdot \exp\left[-i\frac{4\pi}{\lambda}R(t;r_s)\right] \quad (5)$$

where, r_S is the slant-range when the antenna is

Table 1. RADARSAT-1 parameters used for simulated SAR images

parameters	value
Operating frequency	5.3 GHz
Radar wavelength	0.0566 m
Chirp duration time	41.74 μs
Pulse Repetition frequency	1256.98 Hz
Effective Azimuth Antenna Dimension	15 m
Satellite Height	798.5 km
Pulse bandwidth	30.111 MHz
Sampling frequency	32.317 MHz
Pulse center frequency	0 MHz
Satellite velocity	7062 m/s
Data window start time	6.5956 m/s
Azimuth FM rate	1733 Hz/s

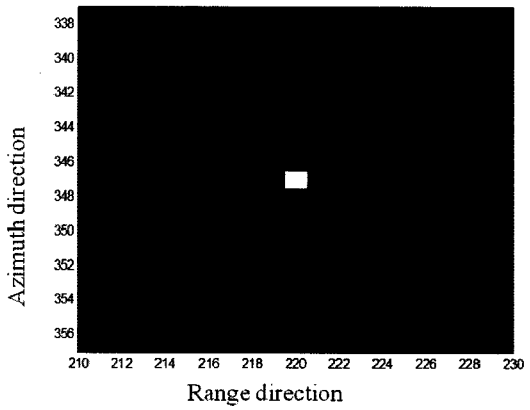

Fig. 3. Simulated SAR image of stationary target without sea clutter background.

abeam of the target, σ is RCS of the target, $R(t; r_S)$ is the slant-range distance at azimuth time t. The antenna weighting in the azimuth direction is denoted by $a(t; r_S)$, and the received signal can be derived as a function of such that

$$s_o\left[\tau - \frac{2R(t;r_s)}{c}\right] = \exp\left[i \cdot \pi \cdot \left\{k \cdot \left(\tau - \frac{2R(t;r_s)}{c}\right)^2\right\}\right] \quad (6)$$

Fig. 3 shows SAR image generated by supposing a stationary vessel that has RCS(σ) of 15dBsm, and the sea clutter is not considered.

4. Application of Velocity Estimation Algorithm to Generated SAR Raw Data

The Doppler frequency of signal in the azimuth direction is altered according to Doppler center frequency f_{DC} and Doppler rate f_R, and these values are calculated using following formula.

$$f_{DC}(r_s) = \frac{2 \cdot V(r_s)}{\lambda} \cdot \sin[\theta_{sq}(r_s)] \quad (7)$$

$$f_R(r_s) = \frac{2 \cdot V^2(r_s)}{\lambda} \cdot \cos^2[\theta_{sq}(r_s)] \quad (8)$$

where, ϕ_{sq} is the squint angle, and $V(r_s)$ is the slant

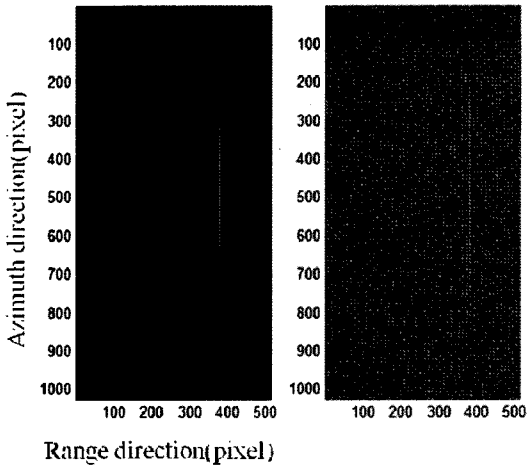

Fig. 4. Range-compressed image of a moving target (10 m/s) without the sea clutter (left) and including the sea clutter background (right).

range velocity changed by azimuth time, t.

Range and azimuth compression processes are carried out by producing matched filters in the range direction using the transmitted chirp pulse, and in the azimuth direction using Doppler center frequency and Doppler rate. This matched filtering process is the standard procedure for the range-Doppler algorithm.

Fig. 4 shows the images after range compression of a moving target at the speed of 10m/s in the range direction whether the sea clutter background is considered or not. Here, the target and sea clutter have RCS(σ) of 15dBsm and -10~10dBsm, respectively.

The velocity estimation mentioned above is first applied to the range-compressed image without the sea clutter. Fig. 5 displays the wrapped and unwrapped phases of azimuth differential data for the left image of Fig. 4 from equation (4). As can be seen from the Fig., the signal from the target extends over approximately 600 pixels which equal Δt (1 pixel = 1/PRF). Therefore, the slant of phase difference in the figure is -10.15 rad/sec, and it is figured out that the Doppler rate from formula (8) is -2133 Hz/s.

Fig. 6 is a result of the moving target's velocity

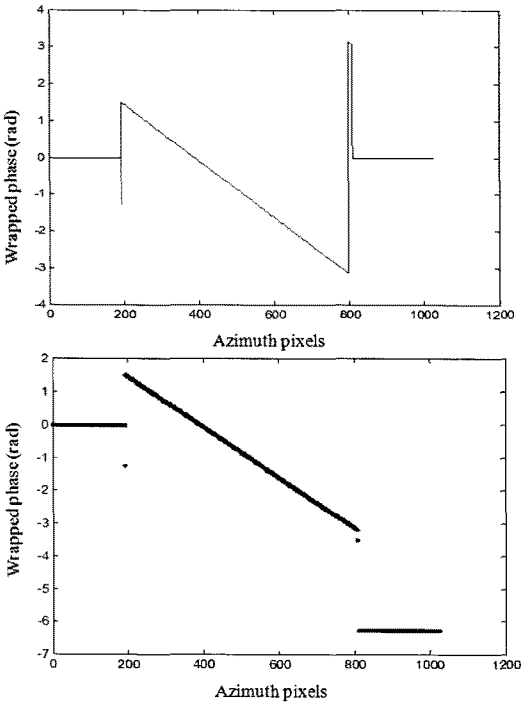

Fig. 5. Wrapped (top) and unwrapped (bottom) phases for azimuth differential data (without sea clutter).

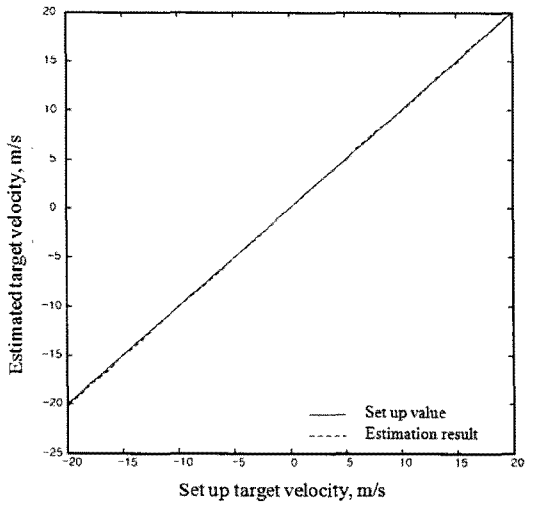

Fig. 6. Comparison of velocity estimations with input true values (without sea clutter).

measurement from -20 m/s to 20 m/s as in the left image of Fig. 4. By comparison with the input velocity of the target, the average error of the measured ground-range velocity was 0.0019m/s, and the maximum error was 0.0531 m/s.

Table 2. Velocity estimations for a target with 6-different direction (flight pass = North ↑). Set-up speed (down) and estimated speed (up), (without sea clutter)

velocity (m/s)	Range direction velocity, m/s					
	NE(45) ↗	E(90) →	SE(135) ↘	SW(225) ↙	W(270) ←	NW(315) ↖
0	0.0019 (0)	0.0019 (0)	0.0019 (0)	0.0019 (0)	0.0019 (0)	0.0019 (0)
10 (range direction velocity)	7.1349 (7.071)	9.9545 (10)	6.9576 (7.071)	-7.1307 (-7.071)	-10.0503 (-10)	-6.9535 (-7.071)

Table 2 is the result of simulation of velocity estimation by taking into account the moving directions. The velocity was measured when the moving directions were NE, E, SE, SW, W, NW under the assumption that SAR's flight pass being north, and the result showed that in the case in which the target's velocity was 0m/s, there was error of 0.0019m/s regardless of the target's moving direction, but when the target's velocity was 10m/s, the maximum error was 0.36m/s (SW), and the average error was 0.19m/s. The overestimation occurred at the directions of NE and SW, while the velocity at SW and SE was underestimated.

To consider the real sea conditions, range-compressed image including sea clutter is used here. Fig. 7 represents the wrapped and unwrapped phases, and signal amplitudes of azimuth differential data with sea clutter background (the right image of Fig. 4). The slant of phase difference is -8.32 rad/sec, and the Doppler rate is -1749 Hz/s.

The source of error in the velocity estimation is in the fact that, in the presence of noise, the SNR (signal to noise ratio) decreases in some parts of data and hence the accurate Doppler parameter estimation becomes difficult.

Fig. 8 displays the intensity variation of differential signals with and without sea clutter. The wind speed above 10m from the sea surface was assumed as

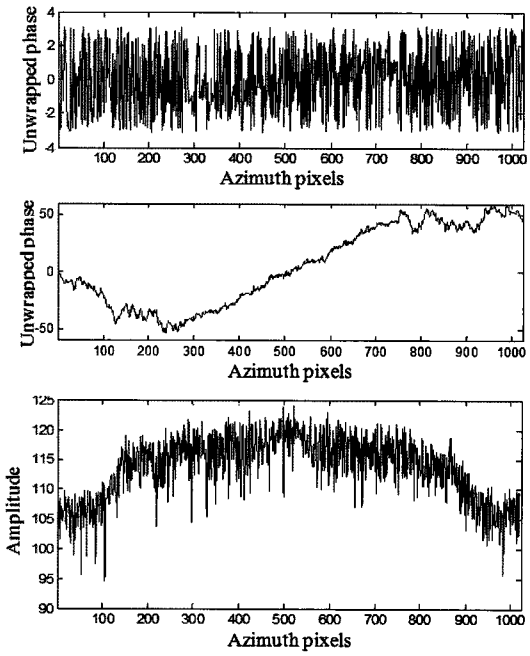

Fig. 7. Wrapped (top) and unwrapped (middle) phases, and magnitude (bottom) for azimuth differential data with sea clutter background.

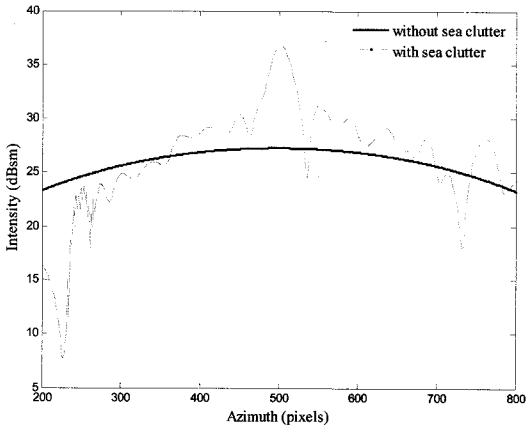

Fig. 8. Intensity of range-compressed differential signals with (dashed line) and without (solid line) sea clutter.

10m/s, and the RCS of the vessel was set as 30 dBsm. If the vessel's RCS is lower than 30 dBsm and the clutter is higher, difficulties in accurate presuming of the target's location occur due to the target's signal hiding effect. This contributes the errors in estimating the Doppler parameter.

In the next, results with sea clutter will be compared for a moving target.

5. The Case of Multiple Scatters

In the above sections, we only considered the case of one moving target in the background of sea clutter. In this section, we consider the case of multiple range moving target at a same azimuth position.

Consider two targets moving toward the west (270 degree) and northward flight direction (Case 1). The targets at the same azimuth position move with the velocity of -10m/s. Case 2 is when a single target is contiguous to the land which has a large RCS of 25dBsm. The movement of the target is the same as Case (1). Case 3 is when surface currents are present.

The results of Cases 1 and 2 are shown in Tables 3 and 4, respectively. In both cases, the error increased as compared with the case of a single target described in the previous sections, and when it was 128 pixels, the error was 1.0m/s or larger.

In Case 3 when ocean currents are present, the motion of principal scatterers on the sea surface affects the phase of the return signals, which can become a source of errors in estimating the velocity of targets. For example, if the surface current velocity in the range direction is set as 3m/s, the estimated phase shift becomes 0.25 rad/s without moving

Table 3. Estimated velocity of two moving targets on the same azimuth line with an identical speed and direction (Case 1)

Distance between two targets (pixels)	512	256	128
Mean error (m/s)	0.16	0.21	0.68
Maximum error (m/s)	0.39	0.40	1.09

Table 4. Estimated velocity of a single moving target and land area on the same azimuth line (Case 2)

Distance between two targets (pixels)	512	256	128
Mean error (m/s)	0.37	0.51	0.85
Maximum error (m/s)	0.56	0.86	1.25

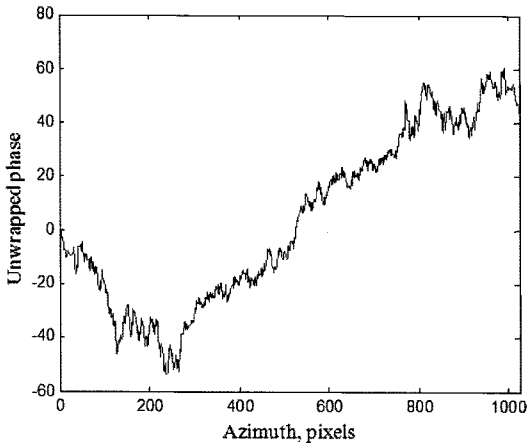

Fig. 9. Phase term of azimuth differential signals with velocity 10 m/s with surface currents moving with 3 m/s to the East.

Table 5. Velocity estimation of a moving target with 10 m/s in the presence of ocean current of 3m/s.

Flight pass: North ↑, Target moving direction: East →				
Sea clutter moving direction	Sea clutter moving direction (range direction velocity, m/s)			
	W ←	NW ↖	NE ↗	E →
Velocity estimation error, m/s	0.82	0.43	0.41	0.79

targets.

Fig. 9 shows the differential phase of the signals from a range moving targets with velocity 10m/s under the current of velocity 3m/s to the east. Compared to the phase of Fig. 7, there exist larger variations in differential phase associated with the background current causing the phase shift of 0.25rad/s.

Table 5 is the result of the velocity measurement of a moving target with 10 m/s to the east in the presence of ocean current of 3m/s.

6. Conculding Remarks

The difference of Doppler centroid frequency caused by moving target can cause the phase difference of azimuth differential signals in SAR image. In this paper, the velocity estimation method of moving target is proposed in SAR system. In order to evaluate the estimation method, simulated moving target signal is generated and the performance is compared with simulated and estimated target velocity. Azimuth difference signals of target and sea clutter are extracted from range compressed SAR images, and extracted wrapped phase is unwrapped for obtaining a phase response which can be converted to azimuth time. For considering real sea environment, the effects of multi-target and coast clutter to have high backscatter coefficient are analysed in term of the error of estimation target velocity. When other moving target or high reflectance clutter is located in 128 pixels, the estimated errors over 1m/s are occurred because other scatters affect azimuth differential signal of moving target. It is noted that estimated velocity of moving target ranges in 1m/s when target exist independently over 256 pixels. This technique may be useful for the surveillance and traffic monitoring of moving ship on the sea and close to the coast.

Acknowledgements

This work was supported by the Basic Research Project, PG47491, of KORDI, "Development of Korea Operational Oceanographic System (KOOS)" funded by the Ministry of Land, Transport and Maritime Affairs of Korean government and the Public Benefit Project of Remote Sensing, "Satellite Remote Sensing for Marine Environment".

References

[1] Graf, K.A. and H. Guthart, 1969. Velocity effects

in synthetic apertures, IEEE Trans. Antennas Propagat., 17: 541-546.

[2] Raney, R.K., 1971. Synthetic aperture imaging radar and moving targets, IEEE Trans. Aerosp. Electron. Syst., 7: 499-505.

[3] Ouchi, K., 2004. Principles of Synthetic Aperture Radar for Remote Sensing, Tokyo Denki University Press: Tokyo.(In Japanese)

[4] Eldhuset, K., 1996. An automatic ship and ship wake detection system for spaceborne SAR images in coastal regions, IEEE Transactions on Geoscience and Remote Sensing, 34(4): 1010-1019.

[5] Wahl, T., K. Eldhuset, and A. Skoelv, 1993. Ship traffic monitoring using the ERS-1 SAR. Proceedings of the First ERS-1 SAR Symposium-Space at the Service of our Environment, Cannes, France, 4-6 November 1992, ESA SP 359: 823-828.

[6] Freeeman, A. and A. Currie, 1987. Synthetic aperture radar (SAR) images of moving targets, GEC Journal of Research, 5(2): 106-115.

[7] Barbarossa, S., 1992. Detection and imaging of moving objects with synthetic aperture radar, IEEE Proceedings-F, 139(1): 79-88, February 1992.

[8] Soumekh, M., 1995. Reconnaissance with ultra wideband UHF synthetic aperture radar, IEEE Signal Processing Magazine, pp.21-40, July 1995.

[9] Werness, S., W. Carrara, L. Joyce, and D. Franczak, 1990. Moving target imaging algorithm for SAR data, IEEE Transactions on Aerospace and Electronic Systems, 26: 57-67.

[10] Young, S., N. Nasrabadi, and M. Soumekh, 1995. SAR moving target detection and identification using stochastic gradient techniques, Proceedings of the International Conference on Acoustics, Speech, and Signal Processing, 4: 2145-2148.

[11] Perry, R., R. DiPietro, and R. Fante, 1999. SAR imaging of moving targets, IEEE Transactions on Aerospace and Electronic Systems, 35(1): 188-200.

[12] Curlander J. C. and R. N. McDonough, 1991. Synthetic Aperture Radar: systems and signal processing, John Wiley & Sons, INC.